Paper 06 / 2026 doi: 10.7795/320.202606

JUNGE wissenschaft

Jungforscher*Innen publizieren
online | *peer reviewed* | original

Verlag:
Physikalisch-
Technische
Bundesanstalt
PTB

Physik

Thickness Identification of 2D Materials by Optical Imaging

Exploring the Relation between Colour and Thickness for $FePS_3$ and $NbSe_2$

This study examines the approach of thickness identification by optical imaging on behalf of a theoretical model and experimental data, using the insulating $FePS_3$ and the conducting $NbSe_2$. The model fits $FePS_3$ data well; expected deviations for $NbSe_2$ were confirmed. An App was created to demonstrate the reliability and practicality of thickness identification by optical imaging for research.

DER JUNGFORSCHER

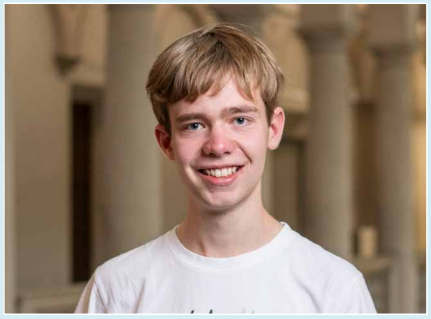

© Schweizer Jugend forscht

Elias Baumann (19)
Realgymnasium Rämibühl,
Zürich

Eingang der Arbeit:
8.8.25
Arbeit angenommen:
25.11.25

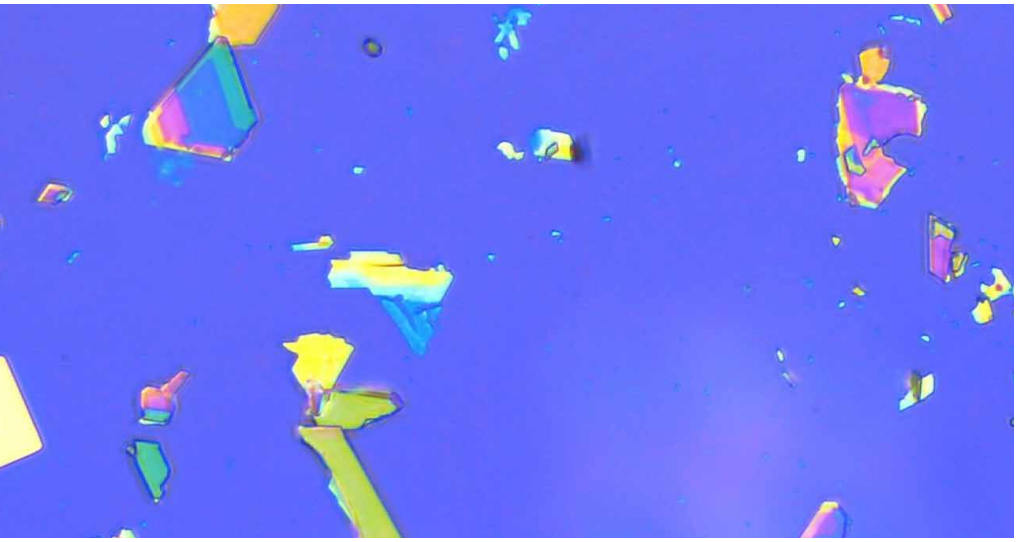

Thickness Identification of 2D Materials by Optical Imaging

Exploring the Relation between Colour and Thickness for $FePS_3$ and $NbSe_2$

1. Introduction

1.1 Two-Dimensional Materials

A two-dimensional (2D) material is a layer of material with a thickness in the nanometre scale. Very often, 2D materials differ from their three-dimensional counterparts not only in size but also in their properties. Due to the exceptional characteristics of 2D materials, such as high conductivity, flexibility and strength, while also being almost transparent, a lot of current research is dedicated to them – especially, since they can be stacked onto each other, creating an unlimited number of combinations of features [1]. Although most 2D materials have only been discovered in recent years, they are not only of great interest for exploring new physical phenomena, but there is a vast range of potential applications, such as optical coatings, drug delivery systems, or water purification [2].

Typically, 2D materials are produced from materials that consist of stacked atom layers. The atoms within one layer are bound together by strong bonds, but the connection between the different layers is caused by much weaker Van der Waals forces. Therefore, these bulk layered materials can be split into small stacks of single layers, then called 2D materials [3]. The separation process is known as exfoliation. Besides mechanical exfoliation, chosen for this investigation since it is very cost and time efficient, other available techniques include chemical vapour deposition, epitaxial growth, or liquid exfoliation [4]. Mechanical exfoliation produces small 2D fragments of material, referred to as flakes, which can be used for experiments.

1.2 Research Question

It was shown that the properties of 2D materials strongly depend on their thickness [3], [5]. In particular, optical properties change significantly with the number of layers. As the (mechanical) exfoliation process results in flakes of various thicknesses, the goal is to develop an application that identifies flakes of a desired thickness in a fast, low-cost, and non-invasive manner. This enables precise and large-scale thickness characterisation to facilitate the production of 2D materials for further research.

Due to the dependence of optical properties on flake thickness, optical characterisation is investigated as an approach for thickness determination. Under white-light illumination, reflection and interference effects from the flakes result in a characteristic optical contrast and colourful appearance [6]. Therefore, this work investigates how the optical contrast and observed colour of a three-layer system, consisting of a thin 2D material flake on a substrate, vary as a function of flake thickness. To address this question, a theoretical model is developed to predict these parameters as a function of thickness. Experimentally, the reflected intensity of the flakes is analysed to determine their optical contrast and RGB values, while their thicknesses are measured independently. By comparing theoretical predictions with experimental results, a thickness-identification application is developed that relates a list of RGB colours of $FePS_3$ flakes to their corresponding thicknesses and used to test whether the results allow to predict thicknesses for exfoliated insulators.

doi: 10.7795/320.202606

1.3 Choice of Materials

Two distinct materials are investigated: Iron phosphorous trisulfide ($FePS_3$) and niobium diselenide ($NbSe_2$). The main difference between the two materials is their electric conductivity. $FePS_3$ is an insulator, while $NbSe_2$ has conductive properties, and can even serve as a superconductor at very low temperatures [5],[7]. They were chosen to examine whether the theoretical model works for insulators, and whether it also holds for conductive materials, regardless of its fundamental assumptions.

The substrate wafers, onto which the flakes are placed after the exfoliation, also play a significant role for the contrast and colour. Conventionally, they are made up of two materials: a 285 nm thick layer of silicon dioxide (SiO_2) on top of 525 µm silicon (Si).

2. Theoretical Model

2.1 Principle of Thickness Identification by Optical Imaging

Observed through an optical microscope, the 2D material flakes appear to have an immense range of colours. The colour of a flake is created by light interference. Due to differences in phase shift for various thicknesses, the wavelengths, for which the reflected rays undergo constructive interference, and the wavelengths, for which destructive interference occurs, are changing with thickness. Thus, measuring the colour of the reflected light encodes the thickness of the flakes. This method has a variety of benefits: it does not require very expensive instruments, it is much faster than an atomic force microscope (AFM) and it does not damage the flakes.

A similar interferometric principle that uses light of various wavelengths to determine the distance between two semi-transparent membranes is well described in literature under the term Fabry–Perot interferometry. For normal incidence, the interference condition depends sensitively on the distance between the membranes, such that small variations in gap thickness lead to measurable shifts in the resonance wavelengths. The resonance wavelengths of a Fabry–Perot interferometer were shown to be highly dependent on this spacing, which supports the precision of thickness determination by optical imaging [6].

In this section, we derive an equation for the expected relative reflectivity r reflected by a three-layer system in dependence of the wavelength of incoming light λ, the thicknesses of both upper layers d_1, d_2 and the refractive indices of all materials involved (similar to [8]). The model is based on Fresnel's Laws, which in turn can be derived directly from Maxwell's equations.

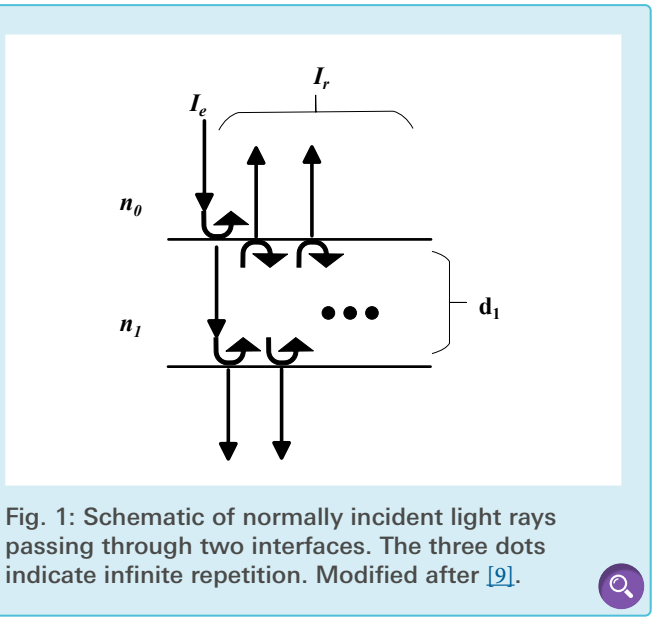

Fig. 1: Schematic of normally incident light rays passing through two interfaces. The three dots indicate infinite repetition. Modified after [9].

2.2 Two Interfaces

If an electromagnetic wave of intensity I_e is incident on a material of small thickness d_1 and refractive index n_1, placed on another material of refractive index $n_2 \neq n_1$, calculating the reflected intensity I_r becomes non-trivial. Figure 1 illustrates the situation for normal incidence: At the first interface, a fraction of the incident ray is reflected, as given by the reflection coefficient r_{01}. The transmitted portion propagates through the upper material n_1, where it may experience absorption, and reaches the second interface. There, part of the ray is further transmitted into the lower material n_2, while the remaining part of it is reflected again as given by r_{12} and travels back toward the first interface. Upon reaching the first interface again, a fraction of this ray is transmitted into the incident medium, contributing to the observable reflected intensity I_r, while another fraction is reflected back into the layer towards the second interface. In total, three aspects must be accounted for: absorption, interference and repetition until infinity.

2.2.1 Absorption

A part of the transmitted wave is absorbed when travelling through matter. The refractive index n_i is complex and determined experimentally with its complex part accounting for absorption.

2.2.2 Interference

Due to the phenomenon of interference the intensity reflected off the first interface and the intensity resulting from the ray fraction reflected from the second interface and transmitted through the first interface cannot simply be added together: the latter wave has acquired a phase-shift $\Delta\varphi_1$ compared to the first one. We can deduce the phase-shift with the help of

doi: 10.7795/320.202606

Figure 1 and the expression of the wave:

$$\vec{E}_0 e^{i(\vec{k}\vec{z}-\omega t)} \tag{1}$$

Here, $\vec{k}$ $\vec{z}$ denotes the phase of the wave with respect to a certain position z. The phase-shift $\Delta\varphi_1$ is built up in the same way – the phase shift occurs because of a spatial difference. As the wave travels the distance d_1 within the upper material, it picks up a phase shift of $\Delta\phi_1 = \left|\vec{k}_1\right| d_1$. Since $\left|\vec{k}_1\right| = n_1 \left|\vec{k}_0\right| = (2\pi n_1)/\lambda$, where $\vec{k}_0$ corresponds to the original $\vec{k}$ from above, expanding yields:

$$\Delta\phi_1 = \frac{2\pi n_1 d_1}{\lambda} \tag{2}$$

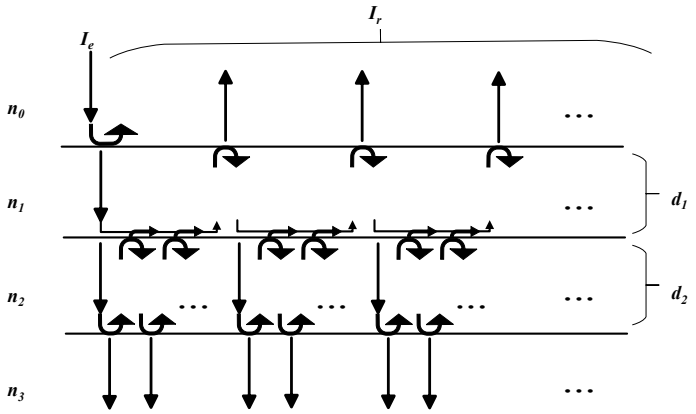

Fig. 2: Model of light rays passing through three interfaces perpendicularly. Three dots indicate infinite repetition. Modified after [8].

2.2.3 Repetition until Infinity

The wave is reflected by both interfaces repeatedly – each time, a smaller fraction of the original ray is transmitted through the first interface into the incident medium and contributes to the total reflected intensity I_r. Let us examine the first few ray fractions reflected out displayed in Figure 1 to illustrate the process. Initially, $r_{tot} \approx r_{01}$. A fraction is transmitted through the first interface (t_{01}), acquires a phase-shift of $\Delta\phi_1$, and some of it is reflected at the second interface (r_{12}). The other fraction of the ray is transmitted and propagates in the lowest medium. As the reflected ray travels up again, it acquires a second phase shift, before most of it is transmitted through the first interface from below (t_{10}). For the moment,

$$r_{tot} \approx r_{01} + t_{01} e^{-i\Delta\phi_1} r_{12} e^{-i\Delta\phi_1} t_{10}. \tag{3}$$

If we continue along the path of the ray fraction, which has travelled once down and up and is not transmitted but reflected (r_{01}), it acquires $\Delta\phi_1$, is reflected again (r_{12}), acquires $\Delta\phi_1$ and is transmitted through the first interface (t_{10}), then

$$r_{tot} \approx r_{01} + t_{01} r_{12} t_{10} e^{-i2\Delta\phi_1} + t_{01} r_{12} r_{10} r_{12} t_{10} e^{-i4\Delta\phi_1} \tag{4}$$

With more and more repetitions:

Equation (5)

Equation (6)

$$r_{tot} = r_{01} + t_{01} r_{12} t_{10} e^{-i2\Delta\phi_1} \sum_{n=0}^{\infty} (r_{10} r_{12} e^{-i2\Delta\phi_1})^n \tag{7}$$

Note that the relative transmissivity $t_{ij} = 1 - r_{ij}$. Applying the formula for an infinite geometric series, since $r_{10} r_{12} e^{-i2\Delta\phi_1} < 1$, and expanding yields the equation for the relative reflectivity of a two-layer system:

$$r_{tot} = r_{01} + \frac{t_{01} r_{12} t_{10} e^{-i2\Delta\phi_1}}{1 - r_{10} r_{12} e^{-i2\Delta\phi_1}} \qquad \therefore$$

$$r_{tot} = \frac{r_{01} + r_{12} e^{-i2\Delta\phi_1}}{1 + r_{01} r_{12} e^{-i2\Delta\phi_1}} \tag{8}$$

$$r_{tot} = r_{01} + t_{01} r_{12} t_{10} e^{-i2\Delta\phi_1} + t_{01} r_{12} r_{10} r_{12} t_{10} e^{-i4\Delta\phi_1} + t_{01} r_{12} r_{10} r_{12} r_{10} r_{12} t_{10} e^{-i6\Delta\phi_1} + \ldots$$

Equation (5)

$$r_{tot} = r_{01} + t_{01} r_{12} t_{10} e^{-i2\Delta\phi_1} \times \left(1 + r_{10} r_{12} e^{-i2\Delta\phi_1} + (r_{10} r_{12} e^{-i2\Delta\phi_1})^2 + (r_{10} r_{12} e^{-i2\Delta\phi_1})^3 + \ldots\right)$$

Equation (6)

doi: 10.7795/320.202606

2.3 Three Interfaces

To predict the amount of reflected light from a flake of thickness d_1 on a SiO_2/Si substrate, where the thickness of SiO_2 is denoted by d_2, we extend the same formalism by defining an effective relative reflectivity r'_{12}, which itself again represents a two layer system. Figure 2 visualises this mathematical idea.

$$r_{tot} = \frac{r_{01} + r'_{12}e^{-i2\Delta\phi_1}}{1 + r_{01}r'_{12}e^{-i2\Delta\phi_1}}$$

$$r'_{12} = \frac{r_{12} + r_{23}e^{-i2\Delta\phi_2}}{1 + r_{12}r_{23}e^{-i2\Delta\phi_2}} \tag{9}$$

Plugging in and simplifying yields the final expression for the relative reflectivity of a three-interface system.

$$r_{tot} = \frac{r_{01} + \frac{r_{12}+r_{23}e^{-i2\Delta\phi_2}}{1+r_{12}r_{23}e^{-i2\Delta\phi_2}}e^{-i2\Delta\phi_1}}{1 + r_{01}\frac{r_{12}+r_{23}e^{-i2\Delta\phi_2}}{1+r_{12}r_{23}e^{-i2\Delta\phi_2}}e^{-i2\Delta\phi_1}} \tag{10}$$

Equation (11)

3. Methodology

The thickness and the red, green, and blue intensity values of various flakes of both iron phosphorous trisulfide $FePS_3$ and niobium diselenide $NbSe_2$ were measured. The measurements were used to determine how the optical contrast and the colour of a three-layer system, consisting of thin flakes on SiO_2/Si substrate, change as a function of flake thickness and to acquire data for further applications. To achieve best precision, materials of current procedural standard were used.

3.1 Preparation of Samples

While the protective coating of the substrate chips was stripped using acetone and isopropanol, the 2D flakes were prepared by mechanical exfoliation under a fume hood: A small piece of crystal was placed on adhesive tape using tweezers. The piece was removed from the tape immediately, leaving behind a very small residue on the tape. The tape was then folded together and gently torn apart 8 times. One of the prepared substrate plates was placed onto the adhesive tape and slight pressure was applied to ensure that some material adheres to the substrate. The substrate chip was then quickly lifted off the tape to yield the sample for investigation.

3.2 Obtaining Experimental Data

After the exfoliation and preparation of $FePS_3$ and $NbSe_2$ samples, groups of flakes were recorded using an optical microscope as well as an AFM in contact mode. As the resolution of 2592×1944 pixels is relatively low for the small flakes, images were only taken if the flakes were large enough to allow a colour value to be obtained later on and the flakes were of distinct height (some big flakes have a wavy surface, where the height varies over short distances). All images for data collection were taken with a Leica MC170 HD microscope through the 50X magnification lens (image size: 243 µm × 182 µm, with built-in white light). The white-balance was set using a white test stripe; any shading, sharpening or contrast enhancement was turned off. For the AFM measurements, contact mode and a resolution of 512 × 512 per 30 µm × 30 µm area was used.

3.3 Measuring Colour Values and Computation of Contrast

To obtain the contrast values as a measure of reflected intensity corresponding to each measured thickness, the colour values at a precise position had to be determined first. A Python script was written to facilitate the process of data extraction. The programme extracts the RGB values at a certain point (x,y) in the optical image. The values are averaged and their standard deviation is calculated over a 5 × 5 pixel square to the bottom right of the point (x,y) to prevent outliers. To check whether the measurement had been taken at the intended position, the measured pixels were marked on the image. Finally, the extracted values were copied to Microsoft Excel and the following calculations were performed:

Levelled RGB and greyscale values

$$I_{levelled} = I - s_{av} + S_{av} \tag{12}$$

$$C = \frac{S_{av} - I_{\text{levelled}}}{S_{av}} \tag{13}$$

Where I is the extracted red, green or blue intensity value of a flake, s_{av} the corresponding adjacent substrate value (average of three substrate measurements close-by), and S_{av} the corresponding average of all substrate values. Equation (12) adjusts for brightness variation in the image, while equation (13) computes the relative contrast to the substrate.

$$r_{tot} = \frac{r_{01} + r_{12}e^{-i2\Delta\phi_1} + r_{23}e^{-i2(\Delta\phi_1+\Delta\phi_2)} + r_{01}r_{12}r_{23}e^{-i2\Delta\phi_2}}{1 + r_{01}r_{12}e^{-i2\Delta\phi_1} + r_{01}r_{23}e^{-i2(\Delta\phi_1+\Delta\phi_2)} + r_{12}r_{23}e^{-i2\Delta\phi_2}}$$

Equation (11)

doi: 10.7795/320.202606

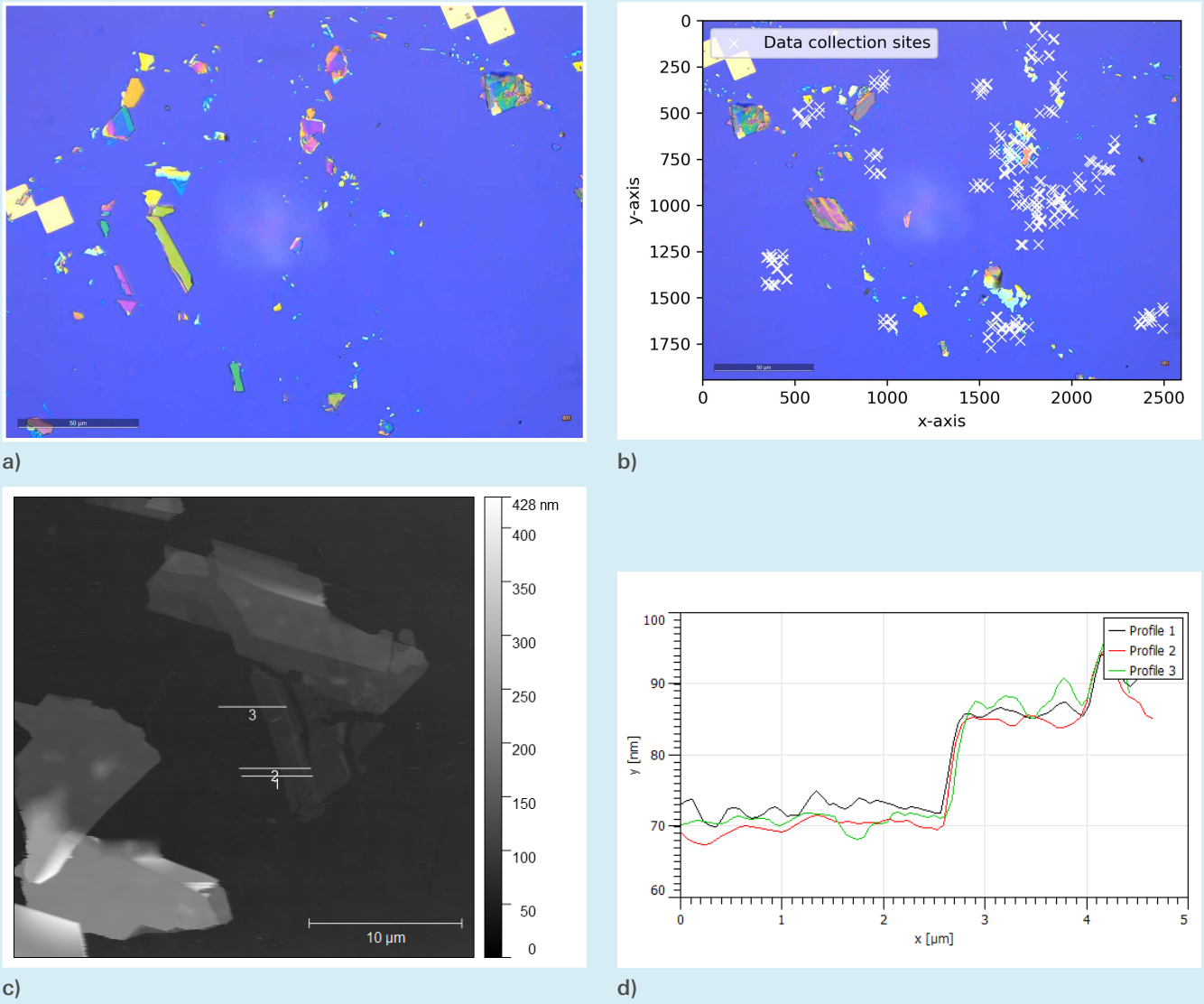

Fig. 3: Exemplary data of $FePS_3$ flakes a) Sample optical microscope image b) RGB data collection sites c) Processed AFM image d) Profiles from AFM image

The relative contrast reduces the effect of specific camera settings and makes the data more comparative with other microscopes. To stay consistent with literature [5] and to allow for better readability, it is simply referred to as contrast.

A measurement as described was attained corresponding to each recorded AFM profile (see below). Additionally, for each AFM image, three similar measurements were done on the close-by substrate to record its brightness (s_{av}). The substate values are used by the application to adapt to different microscopes and light settings.

3.4 Measuring Thickness

The thickness of individual flakes were extracted from AFM images using Gwyddion Version 2.63. The data of the Z-Sensor contains a map of heights that requires processing for more precise results. The maps were levelled using the 'Level data by fitting a plane through three points' feature. The level of the plane was then set to zero such that the displayed height is with respect to the substrate surface.

Profiles of the flake edges were extracted along straight lines in order to measure the thickness of a flake. Each profile extends from the smooth substrate to a flat part of a flake, crossing an edge that is as sharp as possible. The lines were drawn horizontally, following the direction in which the data was recorded to enable high precision. For each flake, three profiles were extracted per area with similar height to reduce the chance of outliers due to measurement errors.

For each AFM image, a graph was produced, showing all extracted profiles (Figure 3d). Using the 'Fit critical dimension' function in Gwyddion, the height of the step in each profile, corresponding to the flake's thickness, and its measurement error were determined and recorded in Microsoft Excel.

doi: 10.7795/320.202606

4. Results

The experimental results were extracted from photos like the ones shown in Figure 3. Both Figure 3a and 3b show a slight blur in the middle of the image and a few darker dots caused by dirt on the lens of the microscope. To prevent outliers, the data was measured in places without such contamination, as indicated in Figure 3b by white crosses.

4.1 Measured Contrast $FePS_3$

From the levelled reflected intensity, obtained by equation (12), the contrast of the flakes with respect to the surrounding substrate for the three colour channels were calculated using the equation (13) and plotted against the AFM measurements of the same flakes (Figure 4). The points were fitted using a damped sinusoidal function of the form

$$C = Ae^{-\lambda d}\cos\left(\omega d + \phi\right) + c \tag{14}$$

where d is the thickness and A, λ, ω, ϕ, c are fitting parameters, yielding r^2 values above 0.83. The resulting fit equations for the red, green, and blue channels are given in equations (15)–(17), respectively.

Red:

$$C = 1.378e^{-d/300.60}\cos\left(\frac{2\pi}{120.25}\cdot d - 0.222\right) - 0.711 \tag{15}$$

Green:

$$C = 1.389e^{-d/114.70}\cos\left(\frac{2\pi}{115.51}\cdot d + 0.700\right) - 0.697 \tag{16}$$

Blue:

$$C = -0.445e^{-d/1020.3}\cos\left(\frac{2\pi}{81.574}\cdot d + 4.359\right) + 0.268 \tag{17}$$

For each channel, the contrast values are interpreted as such: if $C = 0$, then the intensity value is the same as for the surrounding substrate ($I_{R_S} = I_R$). If $C = 1$, then $I_R = 0$; it follows that the intensity value is 0. If $C < 0$, the colour value of the flake is higher than the value of the surrounding substrate. Overall, it follows from equation (13):

$$I_{levelled} = (1 - C)\cdot S_{av}. \tag{18}$$

Tab 1: Maxima and minima of measured contrast $FePS_3$

Colour	Contrast Maxima at *d* in nm	Contrast Minima at *d* in nm
Red	3.0 / 123.3	65.2 / 183.4
Green	99.7	42.0 / 157.5
Blue	65.6 / 147.2	24.8 / 106.4 / 188.0

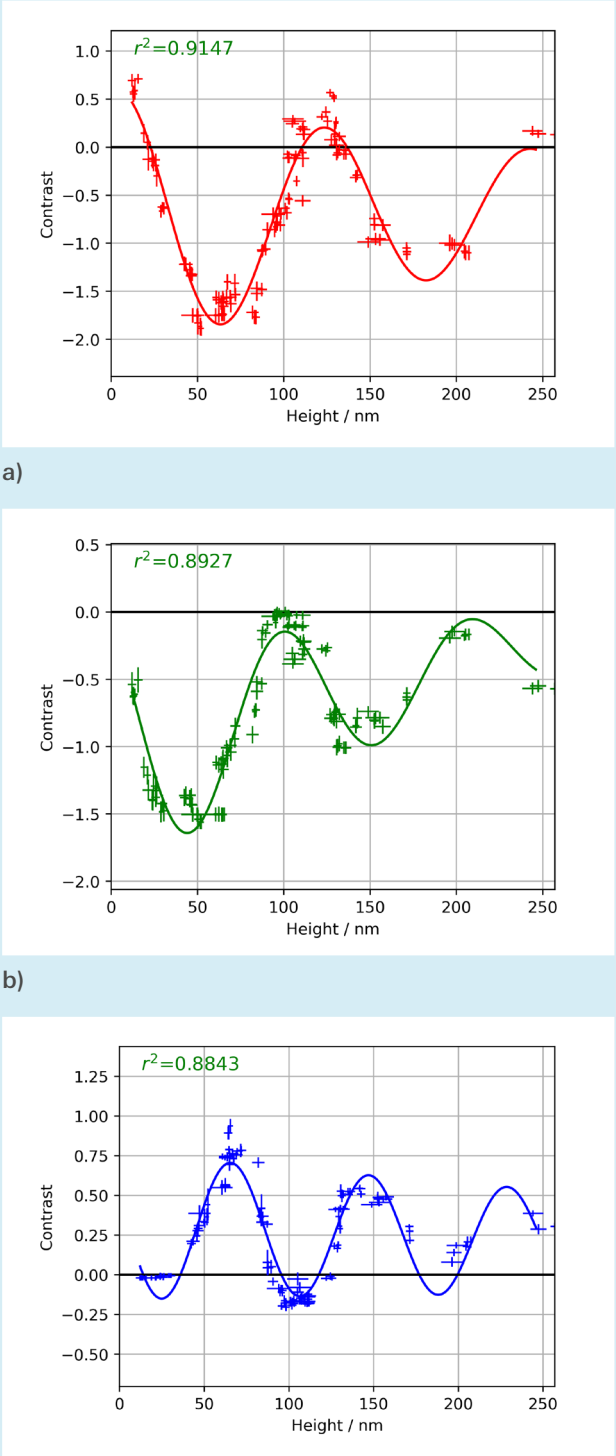

Fig. 4: Measured contrasts for $FePS_3$ plotted over the measured thicknesses with fit for the (a) red, (b) green, and (c) blue color channels

doi: 10.7795/320.202606

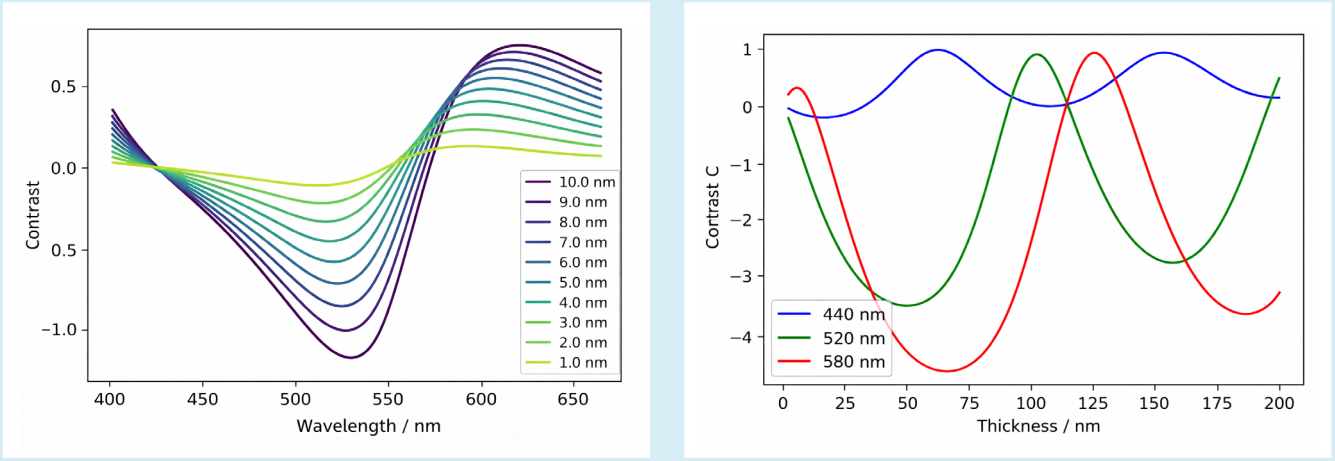

a) b)

Fig. 5: Computing the predicted contrast for $FePS_3$ on Si/SiO_2 substrate (a) per wavelength for 10 thicknesses and (b) per thickness for three wavelengths

To find the contrast minima and maxima, the fit functions were differentiated with respect to d; the zeros of the derivative were computed using a Desmos Scientific Calculator and are shown in the Table 1.

4.2 Computing the Theoretical Model $FePS_3$

Using Python, the equation (11) developed in the Chapter 2, was computed for a thickness range of 1-200 nm for $FePS_3$ on a SiO_2/Si substrate and is shown in Figure 5. All refractive indices were taken from [10].

The contrast $C = (R_s - R)/R_s$ was computed with respect to the surrounding substrate ($R_s = r_{tot} r^*_{tot}$), as defined in equation (8)). For thicknesses 1–10 nm, the results are shown in Figure 5a. For the thinnest flakes, the decrease in contrast at a wavelength of approximately 535 nm and the increase at 630 nm per nm are constant; the contrast changes linearly with the thickness of the flake. Around the blue wavelengths (approximately 420 nm), the contrast is close to 0 and does not vary for thin flakes. The calculated, theoretical contrast for thicknesses between 1 nm and 200 nm is shown in Figure 5b and the corresponding, graphically estimated minima and maxima are given in Table 2.

4.3 Measured Contrast $NbSe_2$

For $NbSe_2$, samples with a thickness of up to 100 nm were investigated. From the raw data, the contrast values were calculated in the same way as for $FePS_3$, according to equation (13), and fitted using a damped sinusoidal function of the form given in equation (14). The measured contrasts for the red, green and blue channels per thickness and the corresponding fits are shown in Figure 6 and the fitted equations are given in equations (19)–(21).

Red:

$$C = 2.577e^{-d/44.02} \cos\left(\frac{2\pi}{128.98} \cdot d + 0.521\right) - 0.741 \quad (19)$$

Green:

$$C = 3.466e^{-d/23.85} \cos\left(\frac{2\pi}{138.07} \cdot d + 0.844\right) - 0.911 \quad (20)$$

Blue:

$$C = -3.161e^{-d/40.15} \cos\left(\frac{2\pi}{1578.43} \cdot d + 1.470\right) + 0.124 \quad (21)$$

The corresponding extrema of the fit functions were determined as: red channel: minimum at 44.9 nm; green channel: minimum at 34.1 nm; blue channel: maximum at 65.1 nm. It must be noted that the r^2 value for the blue channel is relatively low at 0.61; for the other channels, the r^2 value is above 0.88.

4.4 Computing the Theoretical Model for $NbSe_2$

The theoretical model for $NbSe_2$ was computed in the same way as for $FePS_3$, while adapting the refractive index. Since the experimental data was limited to thicknesses below 100 nm, the computations were done for the same range.

Tab 2: Graphically estimated minima and maxima of contrast per thickness for $FePS_3$

Colour	Contrast Maxima at d in nm	Contrast Minima at d in nm
Red	10 / 125	65 / 185
Green	105	50 / 155
Blue	60 / 155	20 / 105 / 195

doi: 10.7795/320.202606

The results of the computations for the theoretically predicted contrast are shown in Figure 7a for the very thin flakes and in Figure 7b with respect to the thickness of the flakes. Note: values close to 1 indicate low intensity, contrast minima correspond to peaks in light intensity.

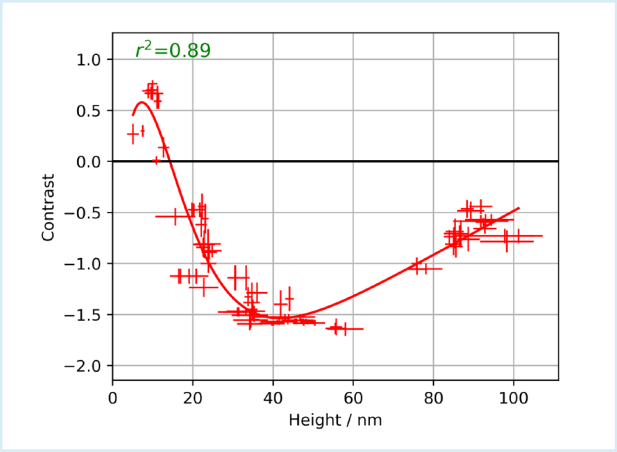

a)

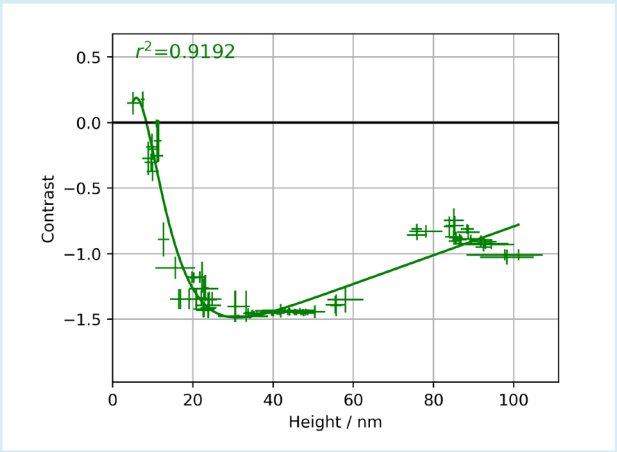

b)

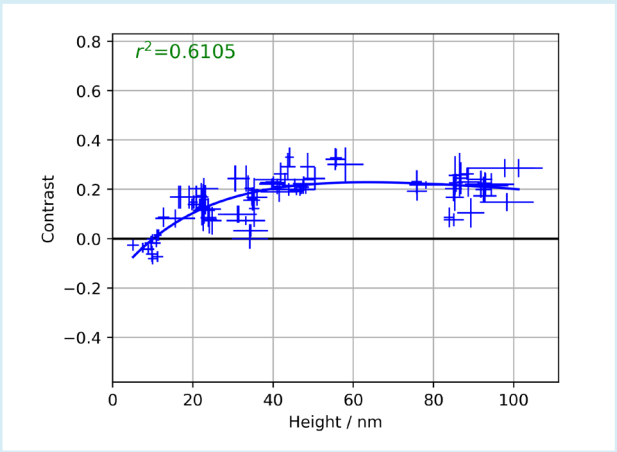

c)

Fig. 6: Measured contrasts for NbSe2 plotted over the measured thicknesses with fit for the (a) red, (b) green, and (c) blue color channels

Again, there is a near linear decrease in contrast for the very thin flakes, especially for wavelengths around 530 nm and 650 nm. Most importantly, in Figure 7b, the green wavelength begins with linearly decreasing contrast up to around 20 nm. It then reaches a minimum of -3.6 just below 50 nm, and continues increasing until 100 nm, even going above 0. The blue wavelength is strong until approximately 35 nm, then the contrast peaks at 60 nm, before decreasing again. Red wavelength is predicted to start with low intensity (0–10 nm), then increase (again, almost linear between 20 nm and 35 nm), peaking at 65 nm thickness and decreasing again. Note that the theory model starts with zero contrast at a thickness of 0 nm.

5. Discussion

5.1 Verification of Theoretical Model

5.1.1 Colours

The colour stripes displayed in Figure 8 provide a way of comparing the results of the experiment and the model. Although this approach is not very precise, it provides an intuitive visualization of the colour-thickness dependence and aids the understanding of the subsequent Figures. Both stripes visualise the corresponding equations (15,16,17), (11) resp.

The key feature of this graph are the thickness values at which colour changes occur. These thicknesses coincide for both the observed and theoretically predicted colours. Around 10 nm, 45 nm, 125 nm, and 165 nm, significant colour changes appear in both colour stripes. To a high degree, the colour progression is also similar, starting from light blue at 10 nm and then changing to yellow and reddish at around 45–80 nm. However, for larger thicknesses the colours begin to deviate: they remain fairly similar up to 125 nm, after which the prediction yields a light blue colour, whereas green was observed.

5.1.2 Contrast

Figure 9 shows a comparison between the measured and the predicted contrast values. Three wavelengths (440 nm, 520 nm, 580 nm) have been selected from the continuous spectrum given by the theoretical model to represent the blue, green, and red colour channels of the camera. The wavelengths have been chosen according to the peak sensitivity of cone cells (which are responsible for colour detection) in the eye [11].

There is a noticeable difference in amplitude between the predicted and measured contrast, especially for the green and red channel. However, this is likely due to spectral characteristics and limited sensitivity of the light source and

doi: 10.7795/320.202606

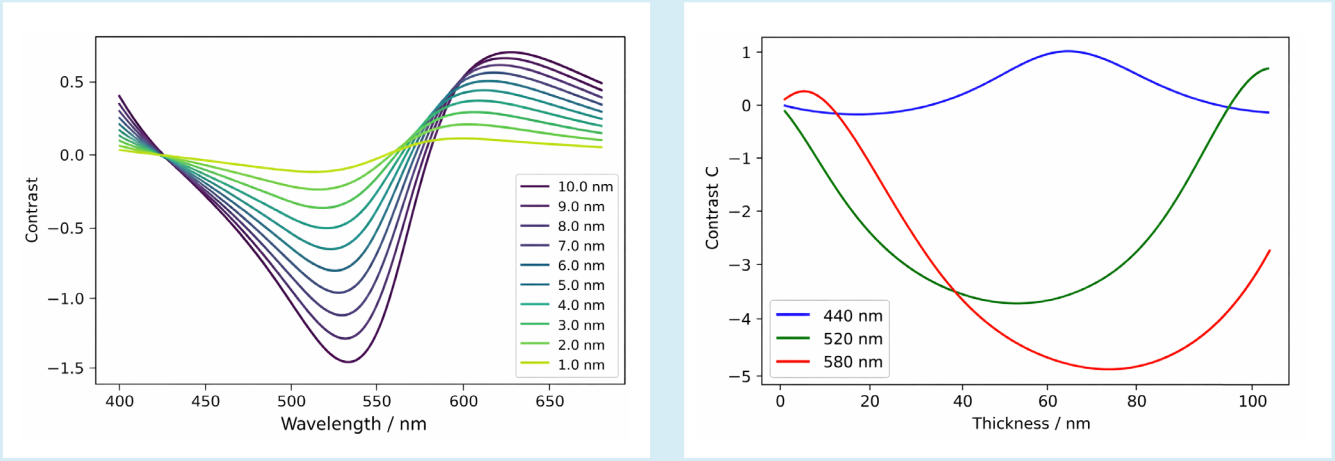

a) b)

Fig. 7: Computing the predicted contrast for $NbSe_2$ on Si/SiO_2 substrate (a) per wavelength for 10 thicknesses and (b) per thickness for three wavelengths

camera sensor in comparison to the uniform incident light spectrum as assumed in the theoretical model. It can easily be calibrated by multiplication with a constant factor.

More relevant is the comparison between the thicknesses, at which the predicted and measured contrast values reach an extrema, and the period at which they are reoccurring: for example, the contrast minimum just above 100 nm for the blue contrast channel coincides precisely; however, the period of the contrast fit functions is smaller, such that the maxima at around 60 nm and 150 nm do not coincide anymore. Similarly for the green channel: the minimum at around 160 nm coincides, but the maximum and the preceding minimum of the predicted and measured contrasts show some deviation. Only for the red channel, the minima coincide precisely, but the maximum is slightly shifted. Therefore, this graph indicates that the selection of three wavelengths in the theoretical model is valid only for a certain range of thicknesses, within which the maxima and minima of the predicted and measured curves align.

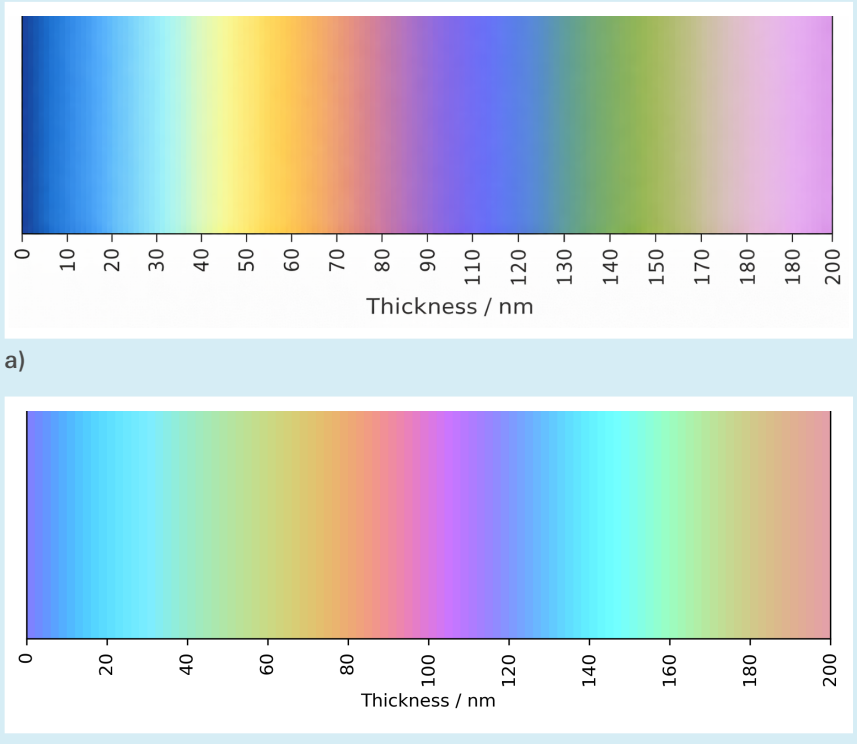

a) b)

Fig. 8: a) Measured and b) predicted colours in dependence of thickness for $FePS_3$

Alternatively, the period of the fit equations may be slightly inaccurate, and future studies could extend the investigated thickness range to 400 nm. However, note that the minima and maxima of the theoretical model depend strongly on the selected wavelengths. Varying them slightly (around 5 nm) already results in a relatively large shift of the thicknesses at which the maxima and minima occur. Since the period of the measured and predicted functions do not coincide exactly, small adjustments of the theoretical wavelengths can be used to configure the theoretical model such that it approximates the contrast for the thickness of interest well. In particular, for the selected wavelengths, quantitative

doi: 10.7795/320.202606

analysis of the minima and maxima yields an average divergence of only 4.5 % between the predicted and measured thicknesses. However, for thicknesses between 50 nm and 155 nm, the divergence is only 3.5 %. Choosing slightly shorter wavelengths would allow a more precise approximation of the smaller thicknesses (down to 1 nm), since interference minimum and maximum are closer together.

5.1.3 Literature Comparison

B. Ma et al. [5] used a similar method for determining the thickness of 2D materials based on optical contrast for different materials (Graphene, hexagonal boron nitride (h-BN) and molybdenum disulfide (MoS_2)). They focused on very thin flakes, ranging from one to ten layers of atoms.

They computed a graph of the optical contrast as a function of wavelength, similar to that shown in Figure 5a. A comparison shows a similar shape: both graphs show a minimum and a maximum - those of h-BN occurring at wavelengths 30-40 nm shorter- as expected, for a material with a slightly lower refractive index than $FePS_3$.

More importantly, both models predict a linear de-/increase of contrast for wavelengths around 500-550 nm for very thin flakes. This is useful for applications, because it allows precise identification of thickness. But: *"Note that the largest layer numbers of [...] h-BN that can be identified through this method is [...] 10, respectively, since the changes of the image contrasts are less and less obvious with further increasing the layer number."* [5] B. Ma et al. reported limitations: after a few layers (in their case 10 layers corresponding to a thickness of about 3 nm), the linearity is no longer preserved. In contrast, for $FePS_3$ on top of a 285 nm layer of SiO_2, the linearity extends to a thickness of at least 30 nm. Allowing for a slight curvature, the range can even extend to around 45 nm, with each layer having its own specific contrast. As described above, the theoretical model can be adjusted such that it fits the very thin flakes precisely.

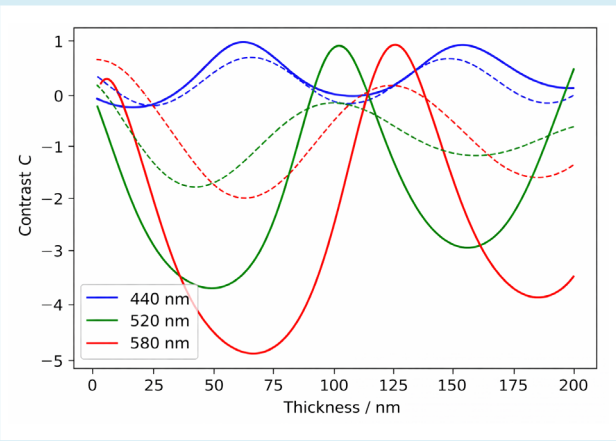

Fig. 9: Measured and predicted contrast in dependence of thickness (solid line: predicted; dashed line: measured)

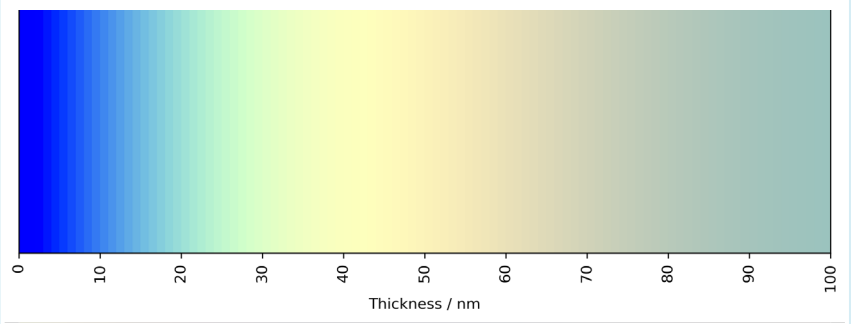

a)

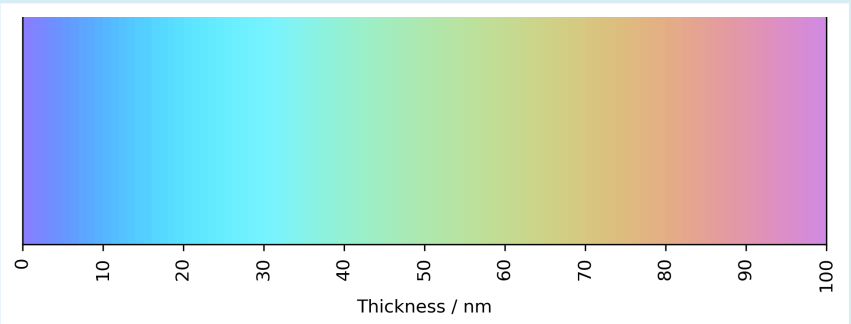

b)

Fig. 10: a) Measured and b) predicted colours in dependence of thickness for $NbSe_2$

5.2 Analysing Results of $NbSe_2$ and Literature Comparison

The experiment described in section 3 was additionally conducted for $NbSe_2$ to examine, whether a significant difference arises, if the top layer of the structure is a metal instead of an insulator. The following comparison between experimental and theoretical results suggests an answer.

The measured and predicted colours are shown in Figure 10. There is a strong deviation in the colour progression: although both start blueish (a very strong blue was measured, more purple was predicted), the light blue ends at a thickness 20 nm lower than in the prediction. Instead, a slow change to a pale yellow occurs. This colour never even appears in the predicted colours -

doi: 10.7795/320.202606

here the progression continues from light blue to greenish to yellow, orange, red and pink. The key difference to the results of $FePS_3$ is that the colour changes do not occur at the same thicknesses. Therefore, the divergence between the predicted and the measured colours is not due to spectral characteristics of the light source and detector. The fact that $NbSe_2$ does not behave as predicted by the theoretical model was also found by M. M. Benameur et al. [6], confirming the observation presented in this report.

Analysing the fit equations reveals why $NbSe_2$ is not suitable for thickness identification by optical imaging from about 75 nm on. The dampening factor λ for $NbSe_2$ is on average 9 times greater than for $FePS_3$. Consequently, the colours approach the colour of 3D $NbSe_2$ quicker, and thus thicker flakes cannot be distinguished precisely.

6. Application and further Ideas

6.1 Production of 2D materials

To conduct experiments with 2D materials, their thickness must be known, as it has a strong influence on the properties [3],[5]. The aim of this section is to develop a precise application, coded using Python, which can convert recorded RGB values into an estimate of thickness, to speed up the process of thickness identification, and assert its reliability.

6.2 Working Principle of the Application

In order to find the corresponding thickness to an input RGB value, firstly, reference RGB values are calculated based on the contrast fit functions, relating thickness to colour for each colour channel for a range of thicknesses (here: 0-200 nm). Again, the equation $I_R = (1 - C) S_{av}$ is applied, where C denotes the fit functions and S_{av} are substrate values, measured specifically on the microscope and lens used. This is a simple but effective calibration to account for light spectrum differences, camera sensors and various microscopes.

From the input RGB value, the difference between the value of each channel and the corresponding reference red, green or blue value is calculated for the whole thickness range. A list, containing the maximum difference of the three channels for each thickness is generated (black curve in Figure 11). The thicknesses associated with the lowest difference can then be identified. The number of units above the lowest difference, up to which the differences are accepted and thicknesses in this range are then indicated, is denoted as cutoff. The higher the cutoff, the more possible thicknesses are indicated. Thus the chance that the correct thickness is in the output increases with the cutoff, but the total number of outputs increases as well.

The principle underlying the application is summarised in Figure 11. On the side of the graph, the input RGB value is shown (blue), the horizontal black line represents the cutoff; the thicknesses where the curved black line lies under the cutoff are output.

6.3 Evaluation of Software - Benefits and Limitations

In order to evaluate the application, Figure 12 was generated using the measured thicknesses and RGB values as inputs. Two kinds of ratios are shown:

Equation (22)

Equation (23)

The uncertainty range (e.g. ±2.5 nm) is used for the classification as identified sample: If the measured thickness is not contained exactly in the output thicknesses, but a thickness, which differs from the measured thickness only by the denoted amount of uncertainty, is included, then the sample is called identified.

Figure 12 shows that approximately 45 % of the output thicknesses are at least as close as ±2.5 nm to the actual thickness. More than 70 % of the output thicknesses are at least as close as ±5.5 nm. Depending on the required precision, the flakes with an indicated thickness in the desired range can then be measured more accurately with further instruments. Nevertheless, thickness identification by optical imaging can reduce the number of measurements needed significantly.

Figure 12 indicates that the quality for cutoffs 0 and 3–4 is similar, while the integrity values are much higher for the larger cutoff of 3–4. If ratified by other research groups, this may increase the utility of the application further.

$$\text{integrity} = \frac{\text{number of correctly identified samples}}{\text{number of inputs}(= 124)}$$

Equation (22)

$$\text{quality} = \frac{\text{number of output thicknesses in uncertainty range}}{\text{number of output thicknesses}}$$

Equation (23)

doi: 10.7795/320.202606

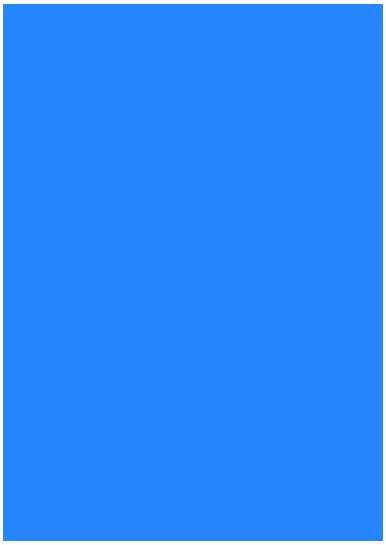

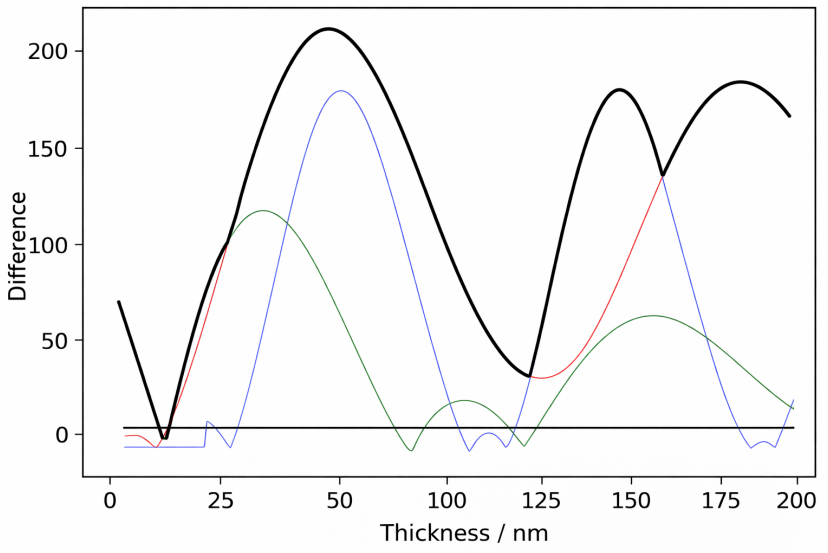

Fig. 11: The application is based on the difference to RGB values; black horizontal line = cutoff; The values were calculated for the colour displayed on the left, representing a possible colour of a flake.

6.4 Outlook

Our application enables one to choose, where on an image the thickness is to be measured, and then generates a list of thicknesses to which the point of interest is likely to correspond. Future versions could be used to analyse images and to indicate flakes of the desired thickness. To fully automatise the identification of flakes of a desired thickness, an optical microscope with a motorised sample platform would be required, allowing the application to scan a whole substrate chip and to yield the positions of flakes of desired thickness. Thus hours of searching for the right flakes can be saved.

Further, if a simple learning algorithm is included after the data fit, which shapes the reference RGB values in more detail, the precision of the application can be enhanced, increasing the precision and utility of thickness identification by optical imaging.

7. Conclusion

In order to investigate, how the optical contrast and the colour depends on the flake thickness and whether the results can be used for thickness determination, a theoretical model was derived from Maxwell's equations, experimental data was collected and evaluated, and a Python script was written to enable the integration of thickness identification by optical imaging in the production workflow of researchers.

Our results confirm that the theoretical model can describe the contrast and colour of an insulator on a two-layered substrate, with average divergences of maxima and minima below 3.5 %. The correlation attests, that the underlying assumptions of the models are well chosen - especially, since there is a significant divergence between the experimental and theoretical results for the conductive material.

From the experimental results of $FePS_3$, an application was developed, which is able to convert a list of RGB values into a

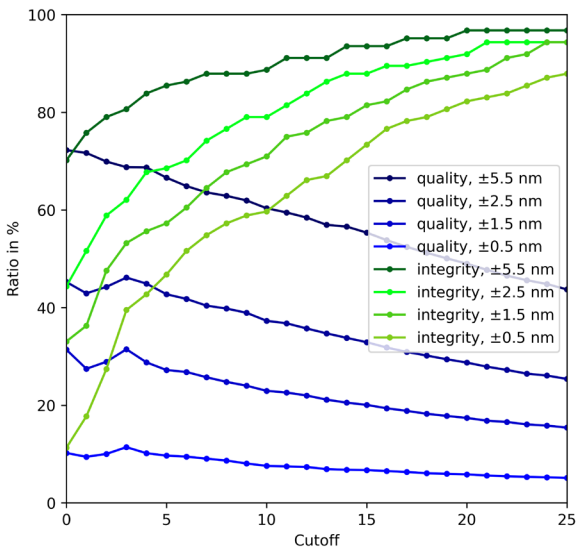

Fig. 12: Integrity and quality per cutoff

doi: 10.7795/320.202606

list of thicknesses, to which the colours correspond very likely. A precision, resulting in above 70 % of the output thicknesses diverging less than ±5.5 nm from the actual height and even 45 % of the output within a range of ±2.5 nm, was achieved. Comparing this to the average standard divergence of the AFM (±2.45 nm), the results confirm the high practicality of thickness identification by optical imaging, providing a fast, non-invasive, large-scale and cheap method to determine the thickness of 2D materials.

Acknowledgements

I would like to express my sincere gratitude to my supervisor Yee Ling Willems-Ong for guiding and supporting me with useful tips and giving very valuable feedback. Additionally, I thank the Department of Materials at ETH Zürich for granting me access to their instruments. Finally, I want to give a special thanks to Niklas Kercher for introducing me to 2D materials, providing me with the opportunity to conduct research in their lab, and answering many of my questions. I am grateful for his patient explanations and his way of giving tips, which motivated me to push even further. I hope that my results and application can contribute to his workflow for the production of 2D materials for his doctorate in magnetism and interface physics.

References

[1] K. S. Novoselov, A. Mishchenko, A. Carvalho, and A. H. Castro Neto. 2D materials and van der Waals heterostructures. Science, 353(6298):aac9439, 2016.
[2] Partha Kumbhakar, Jitha S. Jayan, Athira Sreedevi Madhavikutty, P. R. Sreeram, Appukuttan Saritha, Taichi Ito, and Chandra Sekhar Tiwary. Prospective applications of two-dimensional materials beyond laboratory frontiers: A review. iScience, 26(5):106671, 2023.
[3] Dan Bing, Yingying Wang, Jing Bai, Ruxia Du, Guoqing Wu, and Liyan Liu. Optical contrast for identifying the thickness of two-dimensional materials. Optics Communications, 406:128–138, 2018.
[4] Dattatray J. Late, Bin Liu, H. S. S. Ramakrishna Matte, C. N. R. Rao, and Vinayak P. Dravid. Rapid characterization of ultrathin layers of chalcogenides on SiO_2/Si substrates. Advanced Functional Materials, 22(9):1894–1905, 2012.
[5] Bangjun Ma, Peiqi Wang, Shizhao Ren, Chuancheng Jia, and Xuefeng Guo. Versatile optical determination of two-dimensional atomic crystal layers. Elsevier, 2016.
[6] Parameswaran Hariharan. Basics of Interferometry. Academic Press, 1992.
[7] M. M. Benameur, B. Radisavljevic, J. S. Heron, S. Sahoo, and H. Berger. Visibility of dichalcogenide nanolayers. IOP Science, 2011.
[8] Hugo Anders. Thin Films in Optics. The Focal Press, 1967.
[9] Jordan Edmunds. Thin-film interference using Fresnel equations, 2019.
[10] Refractive index, accessed 7.10.2023.
[11] E. Bruce Goldstein. Sensation and Perception, Seventh Edition. Spektrum Akademischer Verlag, 2007.

doi: 10.7795/320.202606

doi: 10.7795/320.202606

Als Schüler*in wissenschaftlich publizieren

Wie auch aus deiner Wettbewerbsarbeit eine zitierfähige Veröffentlichung wird

Hast du Fragen? In den FAQs auf der Seite „Für Autor*innen“ findest du Antworten.

www.junge-wissenschaft.ptb.de/fuer-autorinnen

Was ist eine wissenschaftliche Veröffentlichung?

Wissenschaftliche Publikationen, sogenannte Papers, sind ein zentrales Element wissenschaftlichen Arbeitens. In Papers werden nicht nur Zeitpunkt und Stand einer Erkenntnis öffentlich dokumentiert, sondern auch mit der Wissenschafts-Community geteilt. So lässt man Kolleg*innen derselben Fachrichtung an Ergebnissen teilhaben oder zeigt progressive Forschungsansätze auf.

Was kostet die Veröffentlichung?

Für die Autor*innen fallen keinerlei Veröffentlichungsgebühren (*page charges*) an. Alle Kosten z. B. für Redaktion, Lektorat, Layout, Website und App tragen Verlag und Sponsoren. Verlag ist die Physikalisch-Technische Bundesanstalt PTB, die das Projekt seit Gründung begleitet.

Was ist besonders an einer wissenschaftlichen Veröffentlichung?

Die Besonderheit eines echten, wissenschaftlichen Papers ist, dass es *peer reviewed* ist. Der Begriff setzt sich zusammen aus den englischen Wörtern *peer* für „Kolleg*in“ und *reviewed* für „überprüft“ (*review* = die Überprüfung). Die Arbeit wird also von einem / einer meist anonymen Fachkolleg*in, der oder dem *referee*, auf Schlüssigkeit überprüft. Die Arbeit ist somit gecheckt und kann als Basis für weitere Forschungsvorhaben genutzt werden.

Wieso wissenschaftlich publizieren?

Diese Papers dienen nicht nur dem fachlichen Austausch, sondern auch als Nachweis der erbrachten Leistungen im jeweiligen Spezialgebiet. Wie ein Lebenslauf informiert die Veröffentlichungsliste über den beruflichen Werdegang und wissenschaftlichen Erfolg.

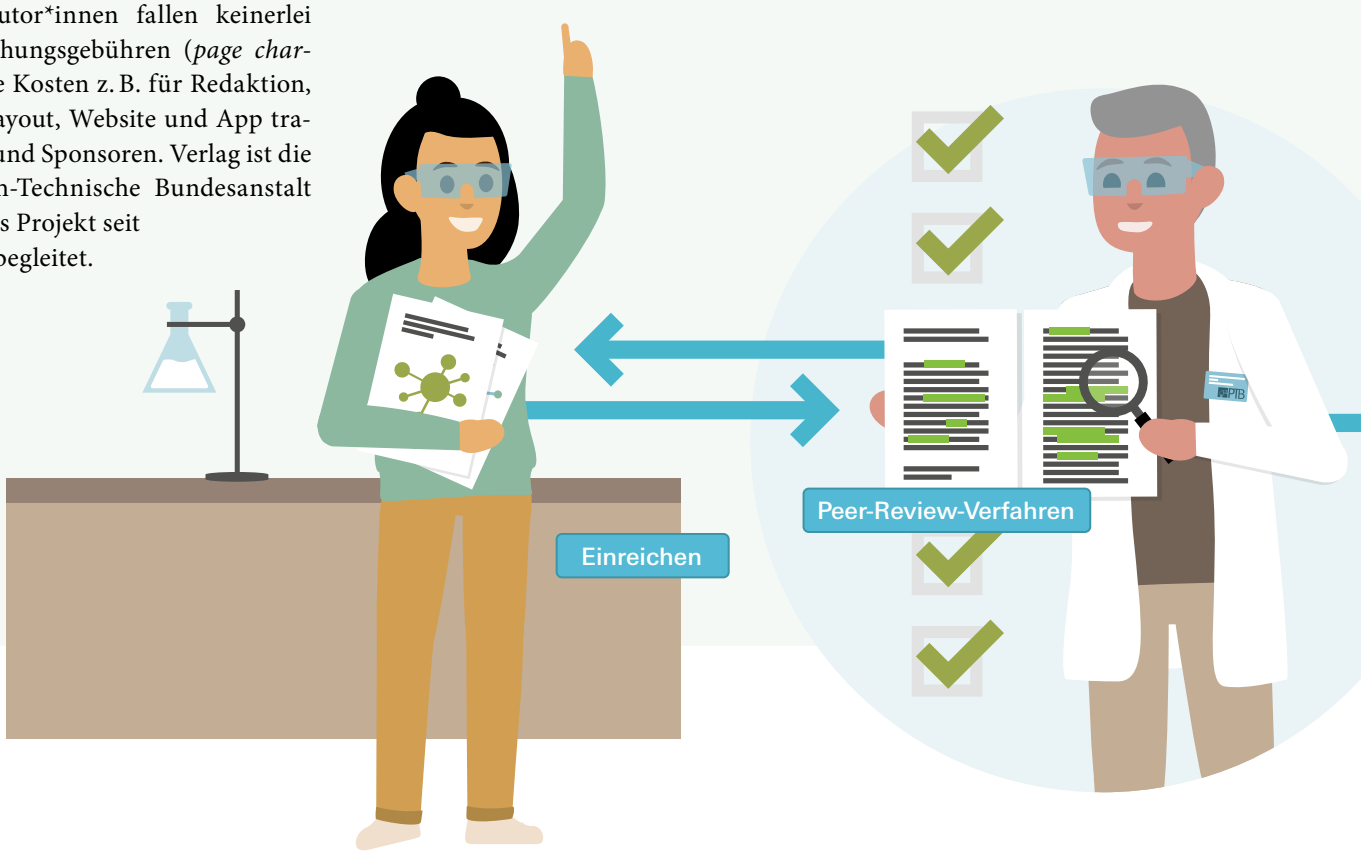

Wie geht das und wie viel Arbeit muss ich investieren?

Die Junge Wissenschaft (JuWi) ist die einzige Plattform, auf der bereits Schüler*innen ein erstes Paper, *peer reviewed*, veröffentlichen können. Das von der JuWi-Chefredaktion eingeleitete und begleitete Peer-Review-Verfahren macht aus deinem Wettbewerbsbeitrag eine zitierfähige Veröffentlichung. Ein JuWi-Paper ist der Startschuss für deine persönliche Veröffentlichungsliste. Und als erfolgreiche Teilnehmer*in eines Forschungswettbewerbs hast du den Löwenanteil der Arbeit bereits erledigt.

Sende deine Arbeit und die Erstveröffentlichungserklärung an:

Chefredaktion
Junge Wissenschaft

Dr.-Ing. Sabine Walter
Paul-Ducros-Straße 7
30952 Ronnenberg

Tel: 05109 / 561508
Mail: sabine.walter@verlag-jungewissenschaft.de

Wie geht es nach dem Einreichen weiter?

Die Chefredakteurin sucht einen geeigneten Fachgutachter*in, der bzw. die, die inhaltliche Richtigkeit der eingereichten Arbeit überprüft und eine Empfehlung ausspricht, ob sie veröffentlicht werden kann (Peer-Review-Verfahren). Das Gutachten wird dir zugeschickt und du erhältst die Möglichkeit, Hinweise des oder der Fachgutachter*in oder eigene Änderungen einzuarbeiten. Die Erfahrung zeigt, dass Arbeiten, die z. B. im Rahmen eines Wettbewerbs wie Jugend forscht die Endrunde erreicht haben, die besten Chancen haben, dieses Peer-Review-Verfahren zu bestehen. Bis hierhin hast du keinerlei Arbeit investiert.

Schließlich kommt die Arbeit in die Redaktion, wird für das Layout vorbereitet und und nach der Freigabe als Open-Access-Beitrag, also für jedermann zugänglich, veröffentlicht.

Was bringt es mir?

JuWi-Autor*innen erwerben in der engen Zusammenarbeit mit der Redaktion Kenntnis über den Aufbau einer wissenschaftlichen Arbeit, über wissenschaftlichen Schreibstil, worauf zu achten ist und welche Schritte wann notwendig sind. Autor*innen eines JuWi-Papers haben so sehr früh einen bedeutenden Teil wissenschaftlichen Publizierens erlernt, noch bevor sie an die Hochschule gehen.

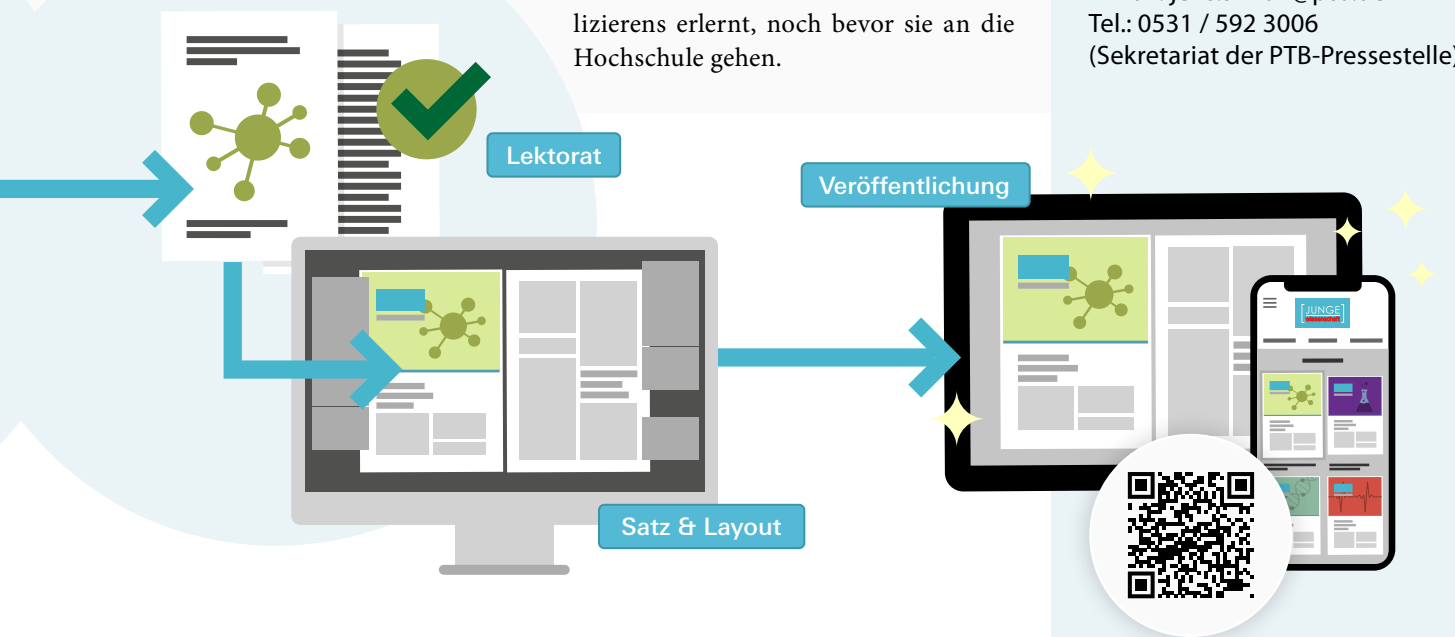

Impressum

Junge Wissenschaft
c/o Physikalisch-Technische Bundesanstalt (PTB)
www.junge-wissenschaft.ptb.de

Redaktion
Dr.-Ing. Sabine Walter,
Chefredaktion Junge Wissenschaft
Paul-Ducros-Str. 7
30952 Ronnenberg
E-Mail: sabine.walter@verlag-jungewissenschaft.de
Tel.: 05109 / 561 508

Sabine Siems, Verlag
E-Mail: sabine.siems@ptb.de
Tel.: 0531 / 592 8202

Design & Satz
Sebastian Baumeister
Art Director / stilsicher.design
E-Mail: baumeister@stilsicher.design
Tel.: 05142 / 302 99 04

Verlag
Dr. Dr. Jens Simon,
Pressesprecher der PTB
Bundesallee 100
38116 Braunschweig
E-Mail: jens.simon@ptb.de
Tel.: 0531 / 592 3006
(Sekretariat der PTB-Pressestelle)

JUNGE wissenschaft

Dein Ticket zur Wissenschaft

Jungforscher*innen publizieren
online | *peer reviewed* | original

Fahrkarte
zum sofortigen Reiseantritt

Für:
1 Jungforscher*in

Nach:
wissenschaftlich publizieren

Über:
peer reviewed

PTB | Preis: Gratis

Die PTB ist jetzt auch bei Instagram. Auf dem Kanal @ptb.bund findest du auch unsere JuWi-Beiträge.